

A VARIABLE TIMESTEPPING ALGORITHM FOR THE UNSTEADY STOKES/DARCY MODEL

YI QIN*, YANREN HOU†, AND WENLONG PEI‡

Abstract. This report considers a variable step time discretization algorithm proposed by Dahlquist, Liniger and Nevanlinna and applies the algorithm to the unsteady Stokes/Darcy model. Although long-time forgotten and little explored, the algorithm performs advantages in variable timestep analysis of various fluid flow systems, including the coupled Stokes/Darcy model. The paper proves that the approximate solutions to the unsteady Stokes/Darcy model are unconditionally stable due to the G -stability of the algorithm. Also variable time stepping error analysis follows from the combination of G -stability and consistency of the algorithm. Numerical experiments further verify the theoretical results, demonstrating the accuracy and stability of the algorithm for time-dependent Stokes/Darcy model.

Key words. variable time stepping, G -stability, second order, coupled Stokes/Darcy model

AMS subject classifications. 76D05, 76S05, 76D03, 35D05

1. Introduction. Stokes/Darcy model, simulating the coupling between surface and subsurface motion of fluid, deserves great interest in geophysics and related areas. Mathematical theory and numerical schemes for both steady and unsteady Stokes/Darcy model have been well developed in recent years [2, 13, 14, 16, 22, 28, 40]. Nevertheless, time discretization for unsteady Stokes/Darcy model is always a big problem where various timestep algorithms give accuracy and efficiency of computation to different levels. Some simulations use constant timestep, first order, fully implicit scheme for simplicity, e.g. [4, 5, 30, 33, 35, 36], while many others implement higher order, constant timestep algorithms to increase accuracy, e.g. [7, 8, 27, 29, 32]. Moreover, time stepping adaptivity through variable stepsize schemes is an ideal way of solving the conflict between time accuracy and computational complexity. Due to the limitations of the most existing methods (e.g. BDF2 is not a A -stable under increasing stepsize), variable timestepping analysis for the unsteady Stokes/Darcy model is promising but little studied.

To solve this issue, we refer to a one-parameter family of two-step, one-leg method proposed by Dahlquist, Liniger and Nevanlinna (the DLN method) [12] and apply the method to time-dependent Stokes/Darcy model for variable timestep analysis. The DLN algorithm maintains the G -stability [9–11, 19] under any arbitrary sequence of time steps and keeps second order accuracy at same time. To begin with, consider the initial value problem

$$x'(t) = f(t, x(t)), \quad x(0) = x_0, \quad (1.1)$$

where $x : [0, T] \rightarrow \mathbb{R}^d$ and $f : \mathbb{R} \times \mathbb{R}^d \rightarrow \mathbb{R}^d$ are vector-valued functions. Let $\{t_n\}_{n=0}^N$ be the grids on time interval $[0, T]$ and $k_n := t_{n+1} - t_n$ be stepsize. Consequently, we define the stepsize parameter $\varepsilon_n \in (-1, 1)$ to be

$$\varepsilon_n = \frac{k_n - k_{n-1}}{k_n + k_{n-1}}.$$

Now given the two initial value x_0 and x_1 , the one parameter DLN algorithm (with parameter $\theta \in [0, 1]$) for the problem (1.1) is

$$\sum_{j=0}^2 \alpha_j x_{n-1+j} = (\alpha_2 k_n - \alpha_0 k_{n-1}) f \left(\sum_{j=0}^2 \beta_{j,n} t_{n-1+j}, \sum_{j=0}^2 \beta_{j,n} x_{n-1+j} \right), \quad (1.2)$$

*School of Mathematics and Statistics, Xi'an Jiaotong University, Xi'an, Shaanxi 710049, China. Email: qinyi1991@stu.xjtu.edu.cn. Subsidized by NSFC (grant No.11971378) and China Scholarship Council grant 201806280136.

†School of Mathematics and Statistics, Xi'an Jiaotong University, Xi'an, Shaanxi 710049, China. Email: yrhou@mail.xjtu.edu.cn. Subsidized by NSFC (grant No.11971378) and China Scholarship Council grant 201806280136.

‡Department of Mathematics, University of Pittsburgh, Pittsburgh, PA 15260, USA. Email: wep17@pitt.edu. Partially supported by NSF grant DMS 1817542.

where coefficients $\{\alpha_j\}_{j=0:2}$ (time-independent) and coefficients $\{\beta_{j,n}\}_{j=0:2}$ (time-dependent) are

$$\begin{bmatrix} \alpha_2 \\ \alpha_1 \\ \alpha_0 \end{bmatrix} = \begin{bmatrix} \frac{\theta+1}{2} \\ \theta \\ \frac{\theta-1}{2} \end{bmatrix}, \quad \begin{bmatrix} \beta_{2,n} \\ \beta_{1,n} \\ \beta_{0,n} \end{bmatrix} = \begin{bmatrix} \frac{1}{4} \left(1 + \frac{1-\theta^2}{(1+\varepsilon_n\theta)^2} + \varepsilon_n^2 \frac{\theta(1-\theta^2)}{(1+\varepsilon_n\theta)^2} + \theta \right) \\ \frac{1}{2} \left(1 - \frac{1-\theta^2}{(1+\varepsilon_n\theta)^2} \right) \\ \frac{1}{4} \left(1 + \frac{1-\theta^2}{(1+\varepsilon_n\theta)^2} - \varepsilon_n^2 \frac{\theta(1-\theta^2)}{(1+\varepsilon_n\theta)^2} - \theta \right) \end{bmatrix}.$$

The coefficients of $\{\alpha_j\}_{j=0:2}$, $\{\beta_{j,n}\}_{j=0:2}$ and the average time step $\alpha_2 k_n - \alpha_0 k_{n-1}$ are constructed to ensure the G -stability and second order accuracy of the method. Combining these fine properties with existing numerical schemes for spatial discretization (e.g. finite element method [17, 24, 34], two grid decoupled method [21, 31, 38, 39, 41], multi-grid decoupled method [1, 37], domain decomposition method [15, 20], etc.), the paper provides with complete variable timestep analysis for unsteady Stokes/Darcy Model (stability and error analysis).

The remainder of the paper is organized as follows: we review the time dependent Stokes/Darcy model (including necessary notations) in section 2. Some preliminaries and two lemmas about properties of the DLN algorithm (1.2) are presented in section 3. In section 4, we apply the variable timestepping DLN algorithm (1.2) to the unsteady Stokes/Darcy model and provide with detailed proofs of unconditional stability and second order convergence of approximate solutions, which are rarely done in other papers. Two numerical tests are given in section 5. The variable timestepping test is aimed to verify the stability of the approximate solutions and followed by a constant timestepping example to confirm the second order convergence by the DLN algorithm.

1.1. Related Works. The variable timestepping analysis on computational fluid flow is little understood due to limitations of the most existing time discretization schemes. The DLN timestepping algorithm, which is second order, unconditionally G -stable under variable time steps, has been applied to the Navier-Stokes equations for variable timestep stability and error analysis [26]. However the first choice for variable timestep analysis of fluid flow is the first order fully implicit method (backward Euler method) for its simplicity and unconditional stability. Recently backward Euler method has been used in artificial compression algorithm with adaptivity for the Navier-Stokes equations [25]. Furthermore it is possible that adding time filters on the backward Euler method increases the order of convergence while keeping the conditional stability for fluid flow [18].

2. The Time-dependent Stokes/Darcy Model. In this section, we consider the unsteady Stokes/Darcy model in region $\Omega = \Omega_f \cup \Omega_p$, where Ω_f is the incompressible fluid region and Ω_p is the porous media region. The two regions are separated by the interface denoted by $\Gamma = \overline{\Omega_f} \cap \overline{\Omega_p}$ and \mathbf{n}_f and \mathbf{n}_p are the unit outward normal vectors on $\partial\Omega_f$ and $\partial\Omega_p$. The schematic representation is displayed in Figure 2.1.

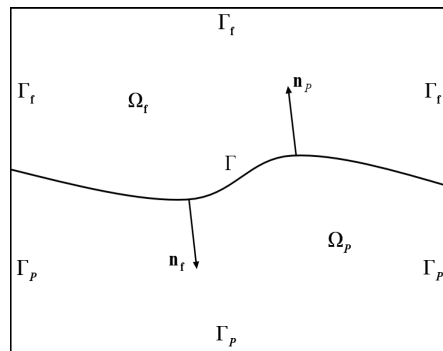


FIG. 2.1. A global domain Ω consisting of a fluid flow region Ω_f and a porous media flow region Ω_p is separated by an interface Γ .

For the finite time interval $[0, T]$, the fluid motion in Ω_f is governed by the time-dependent Stokes equa-

tions, i.e. the fluid velocity $\mathbf{u}_f(\mathbf{x}, t)$ and the pressure $p(\mathbf{x}, t)$ satisfy

$$\begin{aligned} \frac{\partial \mathbf{u}_f}{\partial t} - \nabla \cdot \mathbb{T}(\mathbf{u}_f, p) &= \mathbf{F}_1(\mathbf{x}, t) & \text{in } \Omega_f \times (0, T), \\ \nabla \cdot \mathbf{u}_f &= 0 & \text{in } \Omega_f \times (0, T), \\ \mathbf{u}_f(\mathbf{x}, 0) &= \mathbf{u}_f^0(\mathbf{x}) & \text{in } \Omega_f, \end{aligned} \quad (2.1)$$

where the stress tensor \mathbb{T} and the deformation rate tensor \mathbb{D} are defined as

$$\mathbb{T}(\mathbf{u}_f, p) = -p\mathbb{I} + 2\nu\mathbb{D}(\mathbf{u}_f), \quad \mathbb{D}(\mathbf{u}_f) = \frac{1}{2}(\nabla\mathbf{u}_f + \nabla^{\text{tr}}\mathbf{u}_f)^1.$$

$\nu > 0$ is the kinetic viscosity, \mathbb{I} represents the identity matrix and \mathbf{F}_1 is the external force. The velocity $\mathbf{u}_p(\mathbf{x}, t)$ and hydraulic head $\phi(\mathbf{x}, t)$ in porous media region are governed by the Darcy's law and the saturated flow model

$$\mathbf{u}_p = -\mathbf{K}\nabla\phi \quad \text{in } \Omega_p \times (0, T), \quad (2.2)$$

$$S_0 \frac{\partial \phi}{\partial t} + \nabla \cdot \mathbf{u}_p = F_2(\mathbf{x}, t) \quad \text{in } \Omega_p \times (0, T), \quad (2.3)$$

$$\phi(\mathbf{x}, 0) = \phi^0(\mathbf{x}) \quad \text{in } \Omega_p,$$

where positive symmetric tensor \mathbf{K} denotes the hydraulic conductivity in Ω_p and is allowed to vary in space. S_0 is the specific mass storativity coefficient and F_2 is a source term. Combining (2.2) and (2.3), we obtain the Darcy equation which describes the hydraulic head:

$$S_0 \frac{\partial \phi}{\partial t} - \nabla \cdot (\mathbf{K}\nabla\phi) = F_2(\mathbf{x}, t), \quad \text{in } \Omega_p \times (0, T), \quad (2.4)$$

Now we introduce the boundary conditions:

$$\begin{aligned} \mathbf{u}_f &= 0 \quad \text{on } (\partial\Omega_f \setminus \Gamma) \times (0, T), \\ \phi &= 0 \quad \text{on } (\partial\Omega_p \setminus \Gamma) \times (0, T), \end{aligned} \quad (2.5)$$

and the necessary interface conditions for the coupled Stokes/Darcy model:

$$\begin{aligned} \mathbf{u}_f \cdot \mathbf{n}_f - \mathbf{K}\nabla\phi \cdot \mathbf{n}_p &= 0, & \text{on } \Gamma \times (0, T), \\ -\mathbf{n}_f \cdot (\mathbb{T}(\mathbf{u}_f, p) \cdot \mathbf{n}_f) &= g\phi, & \text{on } \Gamma \times (0, T), \\ -\tau_i \cdot (\mathbb{T}(\mathbf{u}_f, p) \cdot \mathbf{n}_f) &= \frac{\mu_{BJS}\nu\sqrt{d}}{\sqrt{\text{trace}(\Pi)}} \tau_i \cdot \mathbf{u}_f, \quad i = 1, \dots, d-1 & \text{on } \Gamma \times (0, T), \end{aligned} \quad (2.6)$$

where g is the gravitational constant and $\{\tau_i\}_{i=1}^{d-1}$ are the orthonormal system of tangential vectors along Γ . μ_{BJS} is an experimentally determined parameter. Π represents the permeability and satisfies $\mathbf{K} = \frac{\Pi g}{\nu}$.

For weak formulation of the unsteady Stokes/Darcy model, we define some function spaces:

$$\begin{aligned} H_f &= \{\mathbf{v} \in (H^1(\Omega_f))^d : \mathbf{v}|_{\Omega_f \setminus \Gamma} = 0\}, \\ H_p &= \{\psi \in H^1(\Omega_p) : \psi|_{\Omega_p \setminus \Gamma} = 0\}, \\ \mathbf{U} &= H_f \times H_p, \\ Q_f &= L^2(\Omega_f). \end{aligned}$$

We associate the space \mathbf{U} with the following two norms: for all $\underline{\mathbf{v}} = (\mathbf{v}, \psi) \in \mathbf{U}$

$$\begin{aligned} \|\underline{\mathbf{v}}\|_0 &= \sqrt{(\mathbf{v}, \mathbf{v})_{\Omega_f} + gS_0(\psi, \psi)_{\Omega_p}}, \\ \|\underline{\mathbf{v}}\|_{\mathbf{U}} &= \sqrt{\nu(\nabla\mathbf{v}, \nabla\mathbf{v})_{\Omega_f} + g(\mathbf{K}\nabla\psi, \nabla\psi)_{\Omega_p}}, \end{aligned}$$

¹ $\nabla^{\text{tr}}\mathbf{u}_f$ means the transpose of the tensor $\nabla\mathbf{u}_f$.

where $(\cdot, \cdot)_\Omega$ denotes the L^2 -inner product on function space $L^2(\Omega)$. By positive definiteness of tensor \mathbf{K} and Poincaré inequality, there exists constant $C_{0,\mathbf{U}} > 0$ such that

$$\|\underline{\mathbf{v}}\|_0 \leq C_{0,\mathbf{U}} \|\underline{\mathbf{v}}\|_{\mathbf{U}}. \quad (2.7)$$

For convenience, we denote $\|\cdot\|$ and $\|\cdot\|_k$ are norms of L^2 space and Sobolev space H^k respectively.

Now we combine (2.1), (2.4), (2.5) and (2.6) to derive the weak form of time dependent Stokes/Darcy model: given $\mathbf{F} = (\mathbf{F}_1, \mathbf{F}_2) \in L^2(0, T; (L^2(\Omega_f))^d) \times L^2(0, T; L^2(\Omega_p))$, find $\underline{\mathbf{u}}(t) = (\mathbf{u}_f(t), \phi(t)) \in \mathbf{U}$ and $p(t) \in Q_f$ such that for all $\underline{\mathbf{v}} = (\mathbf{v}, \psi) \in \mathbf{U}$, $q \in Q_f$ and any time $t \in (0, T]$

$$\begin{aligned} \left\langle \frac{\partial \underline{\mathbf{u}}}{\partial t}, \underline{\mathbf{v}} \right\rangle_0 + a(\underline{\mathbf{u}}, \underline{\mathbf{v}}) + b(\underline{\mathbf{v}}, p) &= \langle \mathbf{F}, \underline{\mathbf{v}} \rangle_{\mathbf{U}'}, \\ b(\underline{\mathbf{u}}, q) &= 0, \\ \underline{\mathbf{u}}(\mathbf{x}, 0) &= \underline{\mathbf{u}}^0, \end{aligned} \quad (2.8)$$

where

$$\begin{aligned} \left\langle \frac{\partial \underline{\mathbf{u}}}{\partial t}, \underline{\mathbf{v}} \right\rangle_0 &= \left(\frac{\partial \mathbf{u}_f}{\partial t}, \mathbf{v} \right)_{\Omega_f} + g S_0 \left(\frac{\partial \phi}{\partial t}, \psi \right)_{\Omega_p}, \\ a(\underline{\mathbf{u}}, \underline{\mathbf{v}}) &= a_\Omega(\underline{\mathbf{u}}, \underline{\mathbf{v}}) + a_\Gamma(\underline{\mathbf{u}}, \underline{\mathbf{v}}), \\ a_\Omega(\underline{\mathbf{u}}, \underline{\mathbf{v}}) &= a_{\Omega_f}(\mathbf{u}, \mathbf{v}) + a_{\Omega_p}(\phi, \psi), \\ a_{\Omega_f}(\mathbf{u}, \mathbf{v}) &= \nu (\mathbb{D}(\mathbf{u}), \mathbb{D}(\mathbf{v}))_{\Omega_f} + \left(\frac{\mu_{BJS} \nu \sqrt{d}}{\sqrt{\text{trace}(\mathbf{\Pi})}} P_\tau(\mathbf{u}), \mathbf{v} \right)_\Gamma, \\ a_{\Omega_p}(\phi, \psi) &= g (\mathbf{K} \nabla \phi, \nabla \psi)_{\Omega_p}, \\ a_\Gamma(\underline{\mathbf{u}}, \underline{\mathbf{v}}) &= g (\phi, \mathbf{v} \cdot \mathbf{n}_s)_\Gamma - g (\psi, \mathbf{u}_f \cdot \mathbf{n}_s)_\Gamma, \\ b(\underline{\mathbf{v}}, p) &= -(p, \nabla \cdot \mathbf{v})_{\Omega_f}, \\ \langle \mathbf{F}, \underline{\mathbf{v}} \rangle_{\mathbf{U}'} &= \langle \mathbf{F}_1, \mathbf{v} \rangle_{\Omega_f} + g \langle \mathbf{F}_2, \psi \rangle_{\Omega_p}, \\ \underline{\mathbf{u}}^0 &= (\mathbf{u}_f^0(\mathbf{x}), \phi^0(\mathbf{x})). \end{aligned}$$

\mathbf{U}' is the dual space of \mathbf{U} with the norm

$$\|\mathbf{F}\|_{\mathbf{U}'} = \sup_{\underline{\mathbf{v}} \in \mathbf{U} \setminus \{0\}} \frac{\langle \mathbf{F}, \underline{\mathbf{v}} \rangle_{\mathbf{U}'}}{\|\underline{\mathbf{v}}\|_{\mathbf{U}}},$$

and $P_\tau(\cdot)$ is the projection onto the local tangential plane, i.e. $P_\tau(\mathbf{v}) = \mathbf{v} - (\mathbf{v} \cdot \mathbf{n}_s) \mathbf{n}_s$. The bilinear form $a(\cdot, \cdot)$ is continuous and coercive: for all $\underline{\mathbf{u}}, \underline{\mathbf{v}} \in \mathbf{U}$,

$$\begin{aligned} a(\underline{\mathbf{u}}, \underline{\mathbf{v}}) &\leq C_1 \|\underline{\mathbf{u}}\|_{\mathbf{U}} \|\underline{\mathbf{v}}\|_{\mathbf{U}}, \\ a(\underline{\mathbf{u}}, \underline{\mathbf{u}}) &\geq C_2 \|\underline{\mathbf{u}}\|_{\mathbf{U}}^2. \end{aligned} \quad (2.9)$$

Here the above constants $C_1, C_2 > 0$ are independent of functions.

3. Preliminaries. For spatial discretization, we construct regular triangulations of Ω_f and Ω_p with diameter $h > 0$ and choose any finite element spaces $H_{fh} \subset H_f, Q_{fh} \subset Q_f, H_{ph} \subset H_p$ such that the pair (H_{fh}, Q_{fh}) satisfies the discrete LBB^h condition. Typical examples of such pair include Taylor-Hood (P2-P1) and MINI (P1b-P1). Then we define $\mathbf{U}_h = H_{fh} \times H_{ph}$ to be finite element space of \mathbf{U} . The discretely divergence free subspace of H_{fh} is defined to be

$$V_{fh} := \{ \mathbf{v}_h \in H_{fh} : (\nabla \cdot \mathbf{v}_h, q_h) = 0, \forall q_h \in Q_{fh} \},$$

and the divergence free space of \mathbf{U}_h to be $\mathbf{V}_h = V_{fh} \times H_{ph}$.

We define the linear projection operator (see [30]) $P_h = (P_h^{\mathbf{u}}, P_h^p)$ from $\mathbf{U} \times Q_f$ onto $\mathbf{U}_h \times Q_{fh}$: given $t \in (0, T]$ and $(\mathbf{u}(t), p(t)) \in (\mathbf{U}, Q_f)$, $(P_h^{\mathbf{u}}\mathbf{u}(t), P_h^p p(t))$ satisfies

$$\begin{aligned} a(P_h^{\mathbf{u}}\mathbf{u}(t), \mathbf{v}_h) + b(\mathbf{v}_h, P_h^p p(t)) &= a(\mathbf{u}(t), \mathbf{v}_h) + b(\mathbf{v}_h, p(t)), \\ b(P_h^{\mathbf{u}}\mathbf{u}(t), q_h) &= 0. \end{aligned} \quad (3.1)$$

for all $\mathbf{v}_h \in \mathbf{U}_h, q_h \in Q_{fh}$. and the linear projection P_h defined above satisfies

$$\begin{aligned} \|P_h^{\mathbf{u}}\mathbf{u}(t) - \mathbf{u}(t)\|_0 &\leq C_3 h^2 \|\mathbf{u}(t)\|_2, \\ \|P_h^{\mathbf{u}}\mathbf{u}(t) - \mathbf{u}(t)\|_U &\leq C_4 h \|\mathbf{u}(t)\|_2, \\ \|P_h^p p(t) - p(t)\| &\leq C_5 h \|p(t)\|_1. \end{aligned} \quad (3.2)$$

if the pair $(\mathbf{u}(t), p(t))$ is smooth enough.

For the rest of the paper, $P = \{t_n\}_{n=0}^N$ is the partition on time interval $[0, T]$ with $t_0 = 0, t_N = T$ and $k_n = t_{n+1} - t_n$ is the time stepsize. Let \mathbf{u}_h^n, p_h^n denote the approximate solutions of $\mathbf{u}(t_n), p(t_n)$ by the DLN method (1.2) and for convenience, we denote

$$\begin{aligned} \mathbf{u}_{h,\beta}^n &= \beta_{2,n} \mathbf{u}_h^{n+1} + \beta_{1,n} \mathbf{u}_h^n + \beta_{0,n} \mathbf{u}_h^{n-1}, \\ \mathbf{F}_\beta^n &= \beta_{2,n} \mathbf{F}(t_{n+1}) + \beta_{1,n} \mathbf{F}(t_n) + \beta_{0,n} \mathbf{F}(t_{n-1}). \end{aligned}$$

Then we have the discrete weak formulation for the unsteady Stokes/Darcy model by variable timestepping DLN algorithm: given $\mathbf{u}_h^n, \mathbf{u}_h^{n-1}$ and p_h^n, p_h^{n-1} , find $\mathbf{u}_h^{n+1}, p_h^{n+1}$ such that for all $\mathbf{v}_h \in \mathbf{U}_h$ and $q_h \in Q_{fh}$,

$$\begin{aligned} \left\langle \frac{\alpha_2 \mathbf{u}_h^{n+1} + \alpha_1 \mathbf{u}_h^n + \alpha_0 \mathbf{u}_h^{n-1}}{\alpha_2 k_n - \alpha_0 k_{n-1}}, \mathbf{v}_h \right\rangle_0 + a(\mathbf{u}_{h,\beta}^n, \mathbf{v}_h) + b(\mathbf{v}_h, p_{h,\beta}^n) &= \left\langle \mathbf{F}_\beta^n, \mathbf{v}_h \right\rangle_{\mathbf{U}}, \\ b(\mathbf{u}_h^{n+1}, q_h) &= 0. \end{aligned} \quad (3.3)$$

Under LBB^h condition, (3.3) has equivalent form: for all $\mathbf{v}_h \in \mathbf{V}_h$

$$\left\langle \frac{\alpha_2 \mathbf{u}_h^{n+1} + \alpha_1 \mathbf{u}_h^n + \alpha_0 \mathbf{u}_h^{n-1}}{\alpha_2 k_n - \alpha_0 k_{n-1}}, \mathbf{v}_h \right\rangle_0 + a(\mathbf{u}_{h,\beta}^n, \mathbf{v}_h) = \left\langle \mathbf{F}_\beta^n, \mathbf{v}_h \right\rangle_{\mathbf{U}}. \quad (3.4)$$

Before proceeding to next section, we propose two lemmas about the DLN method needed for stability and error analysis.

LEMMA 3.1. *The DLN scheme (1.2) under variable timestep is G-stable, i.e. for any $n = 1, 2, \dots, N-1$, there exist real numbers $\lambda_{j,n}$ ($j = 0, 1, 2$) such that*

$$\left(\sum_{j=0}^2 \alpha_j x_{n-1+j}, \sum_{j=0}^2 \beta_{j,n} x_{n-1+j} \right) = \left\| \begin{matrix} x_{n+1} \\ x_n \end{matrix} \right\|_{G(\theta)}^2 - \left\| \begin{matrix} x_n \\ x_{n-1} \end{matrix} \right\|_{G(\theta)}^2 + \left\| \sum_{j=0}^2 \lambda_{j,n} x_{n-1+j} \right\|^2.$$

Here the $G(\theta)$ -norm $\|\cdot\|_{G(\theta)}$ (timestep independent norm) is

$$\left\| \begin{matrix} y \\ z \end{matrix} \right\|_{G(\theta)}^2 := \frac{1}{4} (1 + \theta) \|y\|^2 + \frac{1}{4} (1 - \theta) \|z\|^2, \quad (3.5)$$

for any $y, z \in \mathbb{R}^d$ and the coefficients $\lambda_{j,n}$ in numerical dissipation are

$$\lambda_{1,n} = -\frac{\sqrt{\theta(1-\theta^2)}}{\sqrt{2}(1+\varepsilon_n\theta)}, \quad \lambda_{2,n} = -\frac{1-\varepsilon_n}{2} \lambda_{1,n}, \quad \lambda_{0,n} = -\frac{1+\varepsilon_n}{2} \lambda_{1,n}.$$

Proof. See [26]. \square

LEMMA 3.2. Let $y : \Omega \times [0, T] \rightarrow \mathbb{R}^d$ be smooth enough, then

$$\left\| \sum_{j=0}^2 \beta_{j,n} y(t_{n-1+j}) - y(t_{n,\beta}) \right\|^2 \leq C(k_n + k_{n-1})^3 \int_{t_{n-1}}^{t_{n+1}} \|y_{tt}\|^2 dt,$$

and for $\theta \in [0, 1)$

$$\left\| \frac{\alpha_2 y(t_{n+1}) + \alpha_1 y(t_n) + \alpha_0 y(t_{n-1})}{\alpha_2 k_n - \alpha_0 k_{n-1}} - y_t(t_{n,\beta}) \right\|^2 \leq C(\theta)(k_n + k_{n-1})^3 \int_{t_{n-1}}^{t_{n+1}} \|y_{ttt}\|^2 dt,$$

where $t_{n,\beta} = \beta_{2,n} t_{n+1} + \beta_{1,n} t_n + \beta_{0,n} t_{n-1}$.

Proof. Apply Taylor theorem with integral reminder to $y(t_{n+1})$, $y(t_{n-1})$ and $y(t_{n,\beta})$ and expand these functions at point t_n . \square

4. Variable timestepping Analysis for the Unsteady Stokes/Darcy Model. Now we apply G -stability of the DLN method (Lemma 3.1) and have the following theorem about stability of approximate solutions by variable timestepping DLN algorithm.

THEOREM 4.1. (*Unconditional Stability*) For any $2 \leq M \leq N$, the approximate solutions of the unsteady Stokes/Darcy model by the algorithm (3.4) satisfy

$$\begin{aligned} & \frac{1}{4}(1+\theta) \|\mathbf{u}_h^M\|_0^2 + \frac{1}{4}(1-\theta) \|\mathbf{u}_h^{M-1}\|_0^2 + \sum_{n=1}^{M-1} \left\| \sum_{j=0}^2 \lambda_{j,n} \mathbf{u}_h^{n-1+j} \right\|_0^2 + C(\theta) \sum_{n=1}^{M-1} (k_n + k_{n-1}) \|\mathbf{u}_{h,\beta}^n\|_U^2 \\ & \leq \frac{1}{4}(1+\theta) \|\mathbf{u}_h^1\|_0^2 + \frac{1}{4}(1-\theta) \|\mathbf{u}_h^0\|_0^2 + \tilde{C}(\theta) \sum_{n=1}^{N-1} (k_n + k_{n-1}) \|\mathbf{F}_\beta^n\|_{U'}^2. \end{aligned} \quad (4.1)$$

Here, the constants $C(\theta), \tilde{C}(\theta) \geq 0$ are independent of the diameter h and time stepsize k_n .

Proof. Let $\mathbf{v}_h = \mathbf{u}_{h,\beta}^n$ in (3.4) and multiply both sides of the equation by $\alpha_2 k_n - \alpha_0 k_{n-1}$,

$$\left\langle \sum_{j=0}^2 \alpha_j \mathbf{u}_h^{n-1+j}, \sum_{j=0}^2 \beta_{j,n} \mathbf{u}_h^{n-1+j} \right\rangle_0 + (\alpha_2 k_n - \alpha_0 k_{n-1}) a(\mathbf{u}_{h,\beta}^n, \mathbf{u}_{h,\beta}^n) = (\alpha_2 k_n - \alpha_0 k_{n-1}) \langle \mathbf{F}_\beta^n, \mathbf{u}_{h,\beta}^n \rangle_{U'}. \quad (4.2)$$

Using Lemma 3.1 for (4.2) and replacing L^2 space by \mathbf{U} and L^2 -norm by $\|\cdot\|_0$ norm, we obtain

$$\left\langle \sum_{j=0}^2 \alpha_j \mathbf{u}_h^{n-1+j}, \sum_{j=0}^2 \beta_{j,n} \mathbf{u}_h^{n-1+j} \right\rangle_0 = \left\| \frac{\mathbf{u}_h^{n+1}}{\mathbf{u}_h^n} \right\|_{G(\theta)}^2 - \left\| \frac{\mathbf{u}_h^n}{\mathbf{u}_h^{n-1}} \right\|_{G(\theta)}^2 + \left\| \sum_{j=0}^2 \lambda_{j,n} \mathbf{u}_h^{n-1+j} \right\|_0^2, \quad (4.3)$$

where $\|\cdot\|_0$ is the norm induced by inner product $\langle \cdot, \cdot \rangle_0$ and the corresponding $G(\theta)$ -norm becomes

$$\left\| \frac{\mathbf{u}_h^{n+1}}{\mathbf{u}_h^n} \right\|_{G(\theta)}^2 = \frac{1}{4}(1+\theta) \|\mathbf{u}_h^{n+1}\|_0^2 + \frac{1}{4}(1-\theta) \|\mathbf{u}_h^n\|_0^2. \quad (4.4)$$

Then we apply (2.9), (4.3) and Cauchy Schwarz inequality to (4.2):

$$\begin{aligned} & \left\| \frac{\mathbf{u}_h^{n+1}}{\mathbf{u}_h^n} \right\|_{G(\theta)}^2 - \left\| \frac{\mathbf{u}_h^n}{\mathbf{u}_h^{n-1}} \right\|_{G(\theta)}^2 + \left\| \sum_{j=0}^2 \lambda_{j,n} \mathbf{u}_h^{n-1+j} \right\|_0^2 + C_2(\alpha_2 k_n - \alpha_0 k_{n-1}) \|\mathbf{u}_{h,\beta}^n\|_U^2 \\ & \leq \frac{C_2}{2} (\alpha_2 k_n - \alpha_0 k_{n-1}) \|\mathbf{u}_{h,\beta}^n\|_{U'}^2 + \frac{1}{2C_2} (\alpha_2 k_n - \alpha_0 k_{n-1}) \|\mathbf{F}_\beta^n\|_{U'}^2. \end{aligned} \quad (4.5)$$

Note that

$$\frac{1-\theta}{2} (k_n + k_{n-1}) \leq \alpha_2 k_n - \alpha_0 k_{n-1} \leq \frac{1+\theta}{2} (k_n + k_{n-1}), \quad (4.6)$$

(4.5) becomes

$$\left\| \frac{\mathbf{u}_h^{n+1}}{\mathbf{u}_h^n} \right\|_{G(\theta)}^2 - \left\| \frac{\mathbf{u}_h^n}{\mathbf{u}_h^{n-1}} \right\|_{G(\theta)}^2 + \left\| \sum_{j=0}^2 \lambda_{j,n} \mathbf{u}_h^{n-1+j} \right\|_0^2 + \frac{C_2(1-\theta)}{4} (k_n + k_{n-1}) \left\| \frac{\mathbf{u}_h^n}{\mathbf{u}_h^\beta} \right\|_{\mathbf{U}}^2 \leq \frac{1+\theta}{4C_2} (k_n + k_{n-1}) \left\| \mathbf{F}_\beta^n \right\|_{\mathbf{U}'}^2. \quad (4.7)$$

Summing over (4.7) from $n = 1, \dots, M-1$ and using (4.4), we obtain (4.1). \square

Next we apply G -stability (Lemma 3.1) and consistency (Lemma 3.2) properties of the DLN algorithm to show the second order convergence of approximate solutions to unsteady Stokes/Darcy model. We denote $\mathbf{u}^n = (\mathbf{u}_f^n, \phi^n)$ and p^n be the exact solutions of the coupled Stokes/Darcy model (2.8) at time t_n and define the error functions to be

$$\begin{aligned} \mathbf{e}^n &= \underline{\mathbf{u}}_h^n - \mathbf{u}^n = (\underline{\mathbf{u}}_h^n - P_h^{\mathbf{u}} \mathbf{u}^n) - (\underline{\mathbf{u}}^n - P_h^{\mathbf{u}} \mathbf{u}^n) = \eta^n - \xi^n, \\ e_p^n &= p_h^n - p^n = (p_h^n - P_h^p p^n) - (p^n - P_h^p p^n) = \eta_p^n - \xi_p^n, \end{aligned} \quad (4.8)$$

and $\eta^0 = \eta^1 = 0$. For variable timestepping analysis, we need to define some continuous and discrete norms. Given $\mathbf{v} \in \mathbf{U}$, $q \in Q_f$, $\mathbf{G} \in \mathbf{U}'$ and $1 \leq m, s < \infty$, we define continuous norms

$$\begin{aligned} \|\mathbf{v}\|_{m,0} &:= \left(\int_0^T \|\mathbf{v}(t)\|_0^m dt \right)^{1/m}, \quad \|\mathbf{v}\|_{m,s} := \left(\int_0^T \|\mathbf{v}(t)\|_s^m dt \right)^{1/m}, \quad \|\mathbf{v}\|_{m,\mathbf{U}} := \left(\int_0^T \|\mathbf{v}(t)\|_{\mathbf{U}}^m dt \right)^{1/m}, \\ \|q\|_{m,L^2} &:= \left(\int_0^T \|q(t)\|^m dt \right)^{1/m}, \quad \|\mathbf{G}\|_{m,\mathbf{U}'} := \left(\int_0^T \|\mathbf{G}(t)\|_{\mathbf{U}'}^m dt \right)^{1/m}. \end{aligned}$$

and new discrete norms

$$\begin{aligned} \|\underline{\mathbf{v}}\|_{m,0} &:= \left(\sum_{n=0}^{N-1} k_n \|\mathbf{v}^{n+1}\|_0^m \right)^{1/m}, \quad \|\underline{\mathbf{v}}\|_{m,s} := \left(\sum_{n=0}^{N-1} k_n \|\mathbf{v}^{n+1}\|_s^m \right)^{1/m}, \\ \|\underline{\mathbf{v}}_\beta\|_{m,s} &:= \left(\sum_{n=0}^{N-1} (k_{n-1} + k_n) \|\mathbf{v}(t_{n,\beta})\|_s^m \right)^{1/m}. \end{aligned}$$

Now we have the main theorem for error analysis.

THEOREM 4.2. (Second order convergence) *The approximate solutions $\{\mathbf{u}_h^n\}_{n=0}^N$ by the variable timestepping DLN scheme (3.4) with parameter $\theta \in [0, 1)$ satisfy*

$$\begin{aligned} \|\underline{\mathbf{u}}_h - \mathbf{u}\|_{2,0} \leq C(\theta) \left\{ \max_{1 \leq n \leq N-1} \{ (k_n + k_{n-1})^2 \} \left(\|p_{tt}\|_{2,L^2} + \|\mathbf{u}_{tt}\|_{2,0} + \|\mathbf{u}_{tt}\|_{2,\mathbf{U}} + \|\mathbf{F}_{tt}\|_{2,\mathbf{U}'} \right) \right. \\ \left. + h^2 \|\underline{\mathbf{u}}_t\|_{2,2} + h^2 \|\underline{\mathbf{u}}\|_{2,2} \right\}, \end{aligned} \quad (4.9)$$

and

$$\begin{aligned} & \left(\sum_{n=1}^{N-1} (\alpha_2 k_n - \alpha_0 k_{n-1}) \left\| \underline{\mathbf{u}}(t_{n,\beta}) - \frac{\mathbf{u}_h^n}{\mathbf{u}} \right\|_{\mathbf{U}}^2 \right)^{1/2} \\ & \leq C(\theta) \max_{1 \leq n \leq N-1} \{ (k_n + k_{n-1})^2 \} \left(\|p_{tt}\|_{2,L^2} + \|\mathbf{u}_{tt}\|_{2,0} + \|\mathbf{u}_{tt}\|_{2,\mathbf{U}} + \|\mathbf{F}_{tt}\|_{2,\mathbf{U}'} \right) + C(\theta) h^2 \|\underline{\mathbf{u}}_t\|_{2,2} \\ & \quad + C(\theta) h \max_{1 \leq n \leq N-1} \{ (k_n + k_{n-1})^2 \} \|\underline{\mathbf{u}}_t\|_{2,2} + C(\theta) h \|\underline{\mathbf{u}}_\beta\|_{2,2}. \end{aligned} \quad (4.10)$$

Proof. By (2.8), the true solutions of unsteady Stokes/Darcy model at time $t_{n,\beta}$. By (2.8) satisfy

$$\left\langle \frac{\partial \underline{\mathbf{u}}}{\partial t}(t_{n,\beta}), \underline{\mathbf{v}}_h \right\rangle_0 + a(\underline{\mathbf{u}}(t_{n,\beta}), \underline{\mathbf{v}}_h) + b(\underline{\mathbf{v}}_h, p(t_{n,\beta})) = \langle \mathbf{F}(t_{n,\beta}), \underline{\mathbf{v}}_h \rangle_{\mathbf{U}'}, \quad \text{for all } \underline{\mathbf{v}}_h \in \mathbf{V}_h. \quad (4.11)$$

Equivalently, (4.11) can be rewritten as

$$\left\langle \frac{\alpha_2 \underline{\mathbf{u}}^{n+1} + \alpha_1 \underline{\mathbf{u}}^n + \alpha_0 \underline{\mathbf{u}}^{n-1}}{\alpha_2 k_n - \alpha_0 k_{n-1}}, \underline{\mathbf{v}}_h \right\rangle_0 + a(\underline{\mathbf{u}}_\beta^n, \underline{\mathbf{v}}_h) + b(\underline{\mathbf{v}}_h, p_\beta^n) = \left\langle \mathbf{F}_\beta^n, \underline{\mathbf{v}}_h \right\rangle_{\mathbf{U}'} + \tau(\underline{\mathbf{u}}(t_{n,\beta}), p(t_{n,\beta}), \underline{\mathbf{v}}_h), \quad (4.12)$$

where

$$\begin{aligned} \underline{\mathbf{u}}_\beta^n &= \beta_{2,n} \underline{\mathbf{u}}^{n+1} + \beta_{1,n} \underline{\mathbf{u}}^n + \beta_{0,n} \underline{\mathbf{u}}^{n-1}, \quad p_\beta^n = \beta_{2,n} p^{n+1} + \beta_{1,n} p^n + \beta_{0,n} p^{n-1}, \\ \tau(\underline{\mathbf{u}}(t_{n,\beta}), p(t_{n,\beta}), \underline{\mathbf{v}}_h) &= \left\langle \frac{\alpha_2 \underline{\mathbf{u}}^{n+1} + \alpha_1 \underline{\mathbf{u}}^n + \alpha_0 \underline{\mathbf{u}}^{n-1}}{\alpha_2 k_n - \alpha_0 k_{n-1}} - \frac{\partial \underline{\mathbf{u}}}{\partial t}(t_{n,\beta}), \underline{\mathbf{v}}_h \right\rangle_0 + a(\underline{\mathbf{u}}_\beta^n - \underline{\mathbf{u}}(t_{n,\beta}), \underline{\mathbf{v}}_h) \\ &\quad + b(\underline{\mathbf{v}}_h, p_\beta^n - p(t_{n,\beta})) - \left\langle \mathbf{F}_\beta^n - \mathbf{F}(t_{n,\beta}), \underline{\mathbf{v}}_h \right\rangle_{\mathbf{U}'}. \end{aligned}$$

Note that $\mathbf{V}_h \subset \mathbf{U}_h$, the system (3.3) holds for all $\underline{\mathbf{v}}_h \in \mathbf{V}_h$. Thus we subtract (4.12) from first equation of (3.3) and use the definition of error function in (4.8) to obtain: for all $\underline{\mathbf{v}}_h \in \mathbf{V}_h$,

$$\begin{aligned} &\left\langle \frac{\alpha_2 \eta^{n+1} + \alpha_1 \eta^n + \alpha_0 \eta^{n-1}}{\alpha_2 k_n - \alpha_0 k_{n-1}}, \underline{\mathbf{v}}_h \right\rangle_0 + a(\eta_\beta^n, \underline{\mathbf{v}}_h) + b(\underline{\mathbf{v}}_h, \eta_{p,\beta}^n) \\ &= \left\langle \frac{\alpha_2 \xi^{n+1} + \alpha_1 \xi^n + \alpha_0 \xi^{n-1}}{\alpha_2 k_n - \alpha_0 k_{n-1}}, \underline{\mathbf{v}}_h \right\rangle_0 + a(\xi_\beta^n, \underline{\mathbf{v}}_h) + b(\underline{\mathbf{v}}_h, \xi_{p,\beta}^n) - \tau(\underline{\mathbf{u}}(t_{n,\beta}), p(t_{n,\beta}), \underline{\mathbf{v}}_h), \end{aligned} \quad (4.13)$$

where

$$\begin{aligned} \eta_\beta^n &= \beta_{2,n} \eta^{n+1} + \beta_{1,n} \eta^n + \beta_{0,n} \eta^{n-1}, \quad \xi_\beta^n = \beta_{2,n} \xi^{n+1} + \beta_{1,n} \xi^n + \beta_{0,n} \xi^{n-1}, \\ \eta_{p,\beta}^n &= \beta_{2,n} \eta_p^{n+1} + \beta_{1,n} \eta_p^n + \beta_{0,n} \eta_p^{n-1}, \quad \xi_{p,\beta}^n = \beta_{2,n} \xi_p^{n+1} + \beta_{1,n} \xi_p^n + \beta_{0,n} \xi_p^{n-1}. \end{aligned}$$

By the definition of discrete divergence free space \mathbf{V}_h and the definition of projection operator P_h , we have

$$b(\underline{\mathbf{v}}_h, \eta_{p,\beta}^n) = 0 \quad \text{and} \quad a(\xi_\beta^n, \underline{\mathbf{v}}_h) + b(\underline{\mathbf{v}}_h, \xi_{p,\beta}^n) = 0. \quad (4.14)$$

Choosing $\underline{\mathbf{v}}_h = \eta_\beta^n$ in (4.13), we apply (4.14) and the Lemma 3.1 to the equation (4.13) to obtain

$$\begin{aligned} &\left\| \frac{\eta^{n+1}}{\eta^n} \right\|_{G(\theta)}^2 - \left\| \frac{\eta^n}{\eta^{n-1}} \right\|_{G(\theta)}^2 + \left\| \sum_{j=0}^2 \lambda_{j,n} \eta^{n-1+j} \right\|_0^2 + C_2(\alpha_2 k_n - \alpha_0 k_{n-1}) \left\| \eta_\beta^n \right\|_{\mathbf{U}}^2 \\ &\leq (\alpha_2 \xi^{n+1} + \alpha_1 \xi^n + \alpha_0 \xi^{n-1}, \eta_\beta^n) - (\alpha_2 k_n - \alpha_0 k_{n-1}) \tau(\underline{\mathbf{u}}(t_{n,\beta}), p(t_{n,\beta}), \eta_\beta^n). \end{aligned} \quad (4.15)$$

Using the Taylor theorem with integral reminder, we have

$$\underline{\mathbf{u}}^n = \underline{\mathbf{u}}^{n+1} + \int_{t_{n+1}}^{t_n} \underline{\mathbf{u}}_t dt, \quad \text{and} \quad \underline{\mathbf{u}}^{n-1} = \underline{\mathbf{u}}^{n+1} + \int_{t_{n+1}}^{t_{n-1}} \underline{\mathbf{u}}_t dt. \quad (4.16)$$

By (4.16) and the fact that $\alpha_2 + \alpha_1 + \alpha_0 = 0$,

$$\begin{aligned} \left\| \alpha_2 \xi^{n+1} + \alpha_1 \xi^n + \alpha_0 \xi^{n-1} \right\|_0 &= \left\| \alpha_1 \int_{t_{n+1}}^{t_n} (P_h^{\underline{\mathbf{u}}} - Id) \underline{\mathbf{u}}_t dt + \alpha_0 \int_{t_{n+1}}^{t_{n-1}} (P_h^{\underline{\mathbf{u}}} - Id) \underline{\mathbf{u}}_t dt \right\|_0 \\ &\leq C(\theta) \int_{t_{n-1}}^{t_{n+1}} \|(P_h^{\underline{\mathbf{u}}} - Id) \underline{\mathbf{u}}_t\|_0 dt, \end{aligned} \quad (4.17)$$

where Id is the identity mapping. Thus by (2.7), (4.17), Cauchy Schwarz inequality and Young's inequality,

$$\left\langle \alpha_2 \xi^{n+1} + \alpha_1 \xi^n + \alpha_0 \xi^{n-1}, \eta_\beta^n \right\rangle_0 \leq C(\theta) \int_{t_{n-1}}^{t_{n+1}} \|(P_h^{\underline{\mathbf{u}}} - Id) \underline{\mathbf{u}}_t\|_0^2 dt + \frac{C_2(\alpha_2 k_n - \alpha_0 k_{n-1})}{2} \left\| \eta_\beta^n \right\|_{\mathbf{U}}^2. \quad (4.18)$$

Summing over (4.15) from $n = 2, \dots, M$ ($2 \leq M \leq N - 1$) and using (4.18),

$$\begin{aligned} & \left\| \frac{\eta^{M+1}}{\eta^M} \right\|_{G(\theta)}^2 - \left\| \frac{\eta^1}{\eta^0} \right\|_{G(\theta)}^2 + \sum_{n=1}^M \left\| \sum_{j=0}^2 \lambda_{j,n} \eta^{n-1+j} \right\|_0^2 + \sum_{n=1}^M \frac{C_2(\alpha_2 k_n - \alpha_0 k_{n-1})}{2} \left\| \eta_\beta^n \right\|_{\mathbf{U}}^2 \\ & \leq C(\theta) \sum_{n=1}^M \int_{t_{n-1}}^{t_{n+1}} \left\| (P_h^{\mathbf{u}} - I) \underline{\mathbf{u}}_t \right\|_0^2 dt - \sum_{n=1}^M (\alpha_2 k_n - \alpha_0 k_{n-1}) \tau \left(\underline{\mathbf{u}}(t_{n,\beta}), p(t_{n,\beta}), \eta_\beta^n \right). \end{aligned} \quad (4.19)$$

Then we deal with four terms of $\tau \left(\underline{\mathbf{u}}(t_{n,\beta}), p(t_{n,\beta}), \eta_\beta^n \right)$ respectively. Combining (2.7), (2.9), Lemma 3.2 and using Cauchy Schwarz inequality, Young's inequality again, we obtain

$$\begin{aligned} & \left\langle \frac{\alpha_2 \underline{\mathbf{u}}^{n+1} + \alpha_1 \underline{\mathbf{u}}^n + \alpha_0 \underline{\mathbf{u}}^{n-1}}{\alpha_2 k_n - \alpha_0 k_{n-1}} - \frac{\partial \underline{\mathbf{u}}}{\partial t}(t_{n,\beta}), \eta_\beta^{n+1} \right\rangle_0 \leq C(\theta) (k_n + k_{n-1})^3 \int_{t_{n-1}}^{t_{n+1}} \left\| \underline{\mathbf{u}}_{tt} \right\|_0^2 dt + \frac{C_2}{16} \left\| \eta_\beta^n \right\|_{\mathbf{U}}^2, \\ & a(\underline{\mathbf{u}}_\beta^n - \underline{\mathbf{u}}(t_{n,\beta}), \eta_\beta^n) \leq C_1 \left\| \underline{\mathbf{u}}_\beta^n - \underline{\mathbf{u}}(t_{n,\beta}) \right\|_{\mathbf{U}} \left\| \eta_\beta^n \right\|_{\mathbf{U}} \leq C(k_n + k_{n-1})^3 \int_{t_{n-1}}^{t_{n+1}} \left\| \underline{\mathbf{u}}_{tt} \right\|_{\mathbf{U}}^2 dt + \frac{C_2}{16} \left\| \eta_\beta^n \right\|_{\mathbf{U}}^2, \\ & b(\eta_\beta^{n+1}, p_\beta^n - p(t_{n,\beta})) \leq C \left\| p_\beta^{n+1} - p(t_{n,\beta}) \right\| \left\| \eta_\beta^n \right\|_{\mathbf{U}} \leq C(k_n + k_{n-1})^3 \int_{t_{n-1}}^{t_{n+1}} \left\| p_{tt} \right\|^2 dt + \frac{C_2}{16} \left\| \eta_\beta^n \right\|_{\mathbf{U}}^2, \\ & \left\langle \mathbf{F}_\beta^n - \mathbf{F}(t_{n,\beta}), \eta_\beta^n \right\rangle_{\mathbf{U}} \leq \left\| \mathbf{F}_\beta^n - \mathbf{F}(t_{n,\beta}) \right\|_{\mathbf{U}} \left\| \eta_\beta^n \right\|_{\mathbf{U}} \leq C(k_n + k_{n-1})^3 \int_{t_{n-1}}^{t_{n+1}} \left\| \mathbf{F}_{tt} \right\|_{\mathbf{U}}^2 dt + \frac{C_2}{16} \left\| \eta_\beta^n \right\|_{\mathbf{U}}^2. \end{aligned} \quad (4.20)$$

Since $\eta^1 = 0 = \eta^0$ and by (3.2), (4.6), the definition of $G(\theta)$ -norm in (3.5), estimators in (4.20), (4.19) becomes

$$\begin{aligned} & \frac{1+\theta}{4} \left\| \eta^{M+1} \right\|_0^2 + \frac{1-\theta}{4} \left\| \eta^M \right\|_0^2 + \sum_{n=1}^M \left\| \sum_{j=0}^2 \lambda_{j,n} \eta^{n-1+j} \right\|_0^2 + \frac{C_2}{4} \sum_{n=1}^M (\alpha_2 k_n - \alpha_0 k_{n-1}) \left\| \eta_\beta^n \right\|_{\mathbf{U}}^2 \\ & \leq C(\theta) \max_{1 \leq n \leq N-1} \{ (k_n + k_{n-1})^4 \} \left(\left\| p_{tt} \right\|_{2,L^2}^2 + \left\| \underline{\mathbf{u}}_{tt} \right\|_{2,0}^2 + \left\| \underline{\mathbf{u}}_t \right\|_{2,\mathbf{U}}^2 + \left\| \mathbf{F}_{tt} \right\|_{2,\mathbf{U}'}^2 \right) + \sum_{n=1}^{N-1} C(\theta) \int_{t_{n-1}}^{t_{n+1}} \left\| (P_h^{\mathbf{u}} - I) \underline{\mathbf{u}}_t \right\|_0^2 dt \\ & \leq C(\theta) \max_{1 \leq n \leq N-1} \{ (k_n + k_{n-1})^4 \} \left(\left\| p_{tt} \right\|_{2,L^2}^2 + \left\| \underline{\mathbf{u}}_{tt} \right\|_{2,0}^2 + \left\| \underline{\mathbf{u}}_t \right\|_{2,\mathbf{U}}^2 + \left\| \mathbf{F}_{tt} \right\|_{2,\mathbf{U}'}^2 \right) + C(\theta) h^4 \left\| \underline{\mathbf{u}} \right\|_{2,2}^2. \end{aligned} \quad (4.21)$$

Using triangle inequality,

$$\left\| \mathbf{e} \right\|_{2,0} \leq \left\| \xi \right\|_{2,0} + \left\| \eta \right\|_{2,0}, \quad (4.22)$$

By (3.2) and (4.21), we have

$$\left\| \xi \right\|_{2,0} = \left(\sum_{n=0}^{N-1} k_n \left\| \xi^{n+1} \right\|_0^2 \right)^{1/2} = \left(\sum_{n=0}^{N-1} k_n \left\| \underline{\mathbf{u}}^n - P_h^{\mathbf{u}} \underline{\mathbf{u}}^n \right\|_0^2 \right)^{1/2} \leq \left(\sum_{n=0}^{N-1} C_3 h^4 k_n \left\| \underline{\mathbf{u}}^{n+1} \right\|_2^2 \right)^{1/2} \leq Ch^2 \left\| \underline{\mathbf{u}} \right\|_{2,2}. \quad (4.23)$$

$$\begin{aligned} \left\| \eta \right\|_{2,0} & \leq C(\theta) \left(\sum_{n=0}^{N-1} k_n \right)^{1/2} \left\{ \max_{1 \leq n \leq N-1} \{ (k_n + k_{n-1})^2 \} \left(\left\| p_{tt} \right\|_{2,L^2}^2 + \left\| \underline{\mathbf{u}}_{tt} \right\|_{2,0}^2 + \left\| \underline{\mathbf{u}}_t \right\|_{2,\mathbf{U}}^2 + \left\| \mathbf{F}_{tt} \right\|_{2,\mathbf{U}'}^2 \right) \right. \\ & \quad \left. + h^2 \left\| \underline{\mathbf{u}} \right\|_{2,2} \right\} \\ & \leq C(\theta) \sqrt{T} \left\{ \max_{1 \leq n \leq N-1} \{ (k_n + k_{n-1})^2 \} \left(\left\| p_{tt} \right\|_{2,L^2}^2 + \left\| \underline{\mathbf{u}}_{tt} \right\|_{2,0}^2 + \left\| \underline{\mathbf{u}}_t \right\|_{2,\mathbf{U}}^2 + \left\| \mathbf{F}_{tt} \right\|_{2,\mathbf{U}'}^2 \right) + h^2 \left\| \underline{\mathbf{u}} \right\|_{2,2} \right\} \end{aligned} \quad (4.24)$$

Combining (4.22), (4.23) and (4.24) results in (4.9). For second part, we have

$$\begin{aligned} & \sum_{n=1}^{N-1} (\alpha_2 k_n - \alpha_0 k_{n-1}) \left\| \mathbf{u}(t_{n,\beta}) - \mathbf{u}_{h,\beta}^n \right\|_{\mathbf{U}}^2 \\ & \leq C(\theta) \sum_{n=1}^{N-1} (k_n + k_{n-1}) \left\| \mathbf{u}(t_{n,\beta}) - \mathbf{u}_{\beta}^n \right\|_{\mathbf{U}}^2 + \sum_{n=1}^{N-1} (\alpha_2 k_n - \alpha_0 k_{n-1}) \left\| \mathbf{u}_{\beta}^n - \mathbf{u}_{h,\beta}^n \right\|_{\mathbf{U}}^2. \end{aligned} \quad (4.25)$$

Using Lemma 3.2,

$$C(\theta) \sum_{n=1}^{N-1} (k_n + k_{n-1}) \left\| \mathbf{u}(t_{n,\beta}) - \mathbf{u}_{\beta}^n \right\|_{\mathbf{U}}^2 \leq C(\theta) \max_{1 \leq n \leq N-1} \{(k_n + k_{n-1})^4\} \|\mathbf{u}_{tt}\|_{2,\mathbf{U}}^2.$$

And

$$\sum_{n=1}^{N-1} (\alpha_2 k_n - \alpha_0 k_{n-1}) \left\| \mathbf{u}_{\beta}^n - \mathbf{u}_{h,\beta}^n \right\|_{\mathbf{U}}^2 \leq C(\theta) \sum_{n=1}^{N-1} (k_n + k_{n-1}) \left\| \xi_{\beta}^n \right\|_{\mathbf{U}}^2 + \sum_{n=1}^{N-1} (\alpha_2 k_n - \alpha_0 k_{n-1}) \left\| \eta_{\beta}^n \right\|_{\mathbf{U}}^2 \quad (4.26)$$

By (3.2) and linearity of the projection operator P_h ,

$$\left\| \xi_{\beta}^n \right\|_{\mathbf{U}}^2 = \left\| P_h^{\mathbf{u}} \mathbf{u}_{\beta}^n - \mathbf{u}_{\beta}^n \right\|_{\mathbf{U}}^2 \leq Ch^2 \left\| \mathbf{u}_{\beta}^n \right\|_2^2 \leq Ch^2 \left\| \mathbf{u}_{\beta}^n - \mathbf{u}(t_{n,\beta}) \right\|_2^2 + Ch^2 \left\| \mathbf{u}(t_{n,\beta}) \right\|_2^2 \quad (4.27)$$

Applying Lemma 3.2 again to (4.27),

$$C(\theta) \sum_{n=1}^{N-1} (k_n + k_{n-1}) \left\| \xi_{\beta}^n \right\|_{\mathbf{U}}^2 \leq C(\theta) h^2 \max_{1 \leq n \leq N-1} \{(k_n + k_{n-1})^4\} \|\mathbf{u}_{tt}\|_{2,2}^2 + C(\theta) h^2 \left\| \mathbf{u}_{\beta} \right\|_{2,2}^2. \quad (4.28)$$

Combining (4.21), (4.25), (4.26) and (4.28), we obtain

$$\begin{aligned} & \sum_{n=1}^{N-1} (\alpha_2 k_n - \alpha_0 k_{n-1}) \left\| \mathbf{u}(t_{n,\beta}) - \mathbf{u}_{h,\beta}^n \right\|_{\mathbf{U}}^2 \\ & \leq C(\theta) \max_{1 \leq n \leq N-1} \{(k_n + k_{n-1})^4\} \left(\|p_{tt}\|_{2,L^2}^2 + \|\mathbf{u}_{tt}\|_{2,0}^2 + \|\mathbf{u}_{tt}\|_{2,\mathbf{U}}^2 + \|\mathbf{F}_{tt}\|_{2,\mathbf{V}}^2 \right) + C(\theta) h^4 \|\mathbf{u}_{tt}\|_{2,2}^2 \\ & \quad + C(\theta) h^2 \max_{1 \leq n \leq N-1} \{(k_n + k_{n-1})^4\} \|\mathbf{u}_{tt}\|_{2,2}^2 + C(\theta) h^2 \left\| \mathbf{u}_{\beta} \right\|_{2,2}^2, \end{aligned}$$

which results in (4.10) \square

5. Numerical Tests. In this section, we use two numerical experiments to verify two distinct properties of the DLN algorithm (stability and consistency). Both numerical tests are implemented by FreeFEM++. The first test confirms that the variable timestepping DLN algorithm is stable for different values of parameter $\theta \in [0, 1]$. In the second experiment, we apply the constant timestepping DLN algorithm to check the second order convergence of the approximate solutions as well as compare it with BDF2 scheme.

5.1. Test of Variable Timestepping DLN algorithm. In this experiment, we use the example mentioned in [3, 23]. Considering the model problem on $\Omega_f = [0, \pi] \times [0, 1]$ and $\Omega_p = [0, \pi] \times [-1, 0]$ with the interface $\Gamma = [0, \pi] \times [0]$:

$$\begin{aligned} \mathbf{u}_f &= \left(\frac{1}{\pi} \sin(2\pi y) \cos(x) e^t, \left(-2 + \frac{1}{\pi^2} \sin(\pi y)^2 \right) \sin(x) e^t \right), \\ p &= 0, \\ \phi &= (e^y - e^{-y}) \sin(x) e^t. \end{aligned}$$

For this test, we set the physical parameters ρ , g , ν , \mathbf{K} , S_0 and μ_{BJS} all equal to 1 and we consider the cases of parameters $\theta = 0.2, 0.5, 0.7$ in DLN scheme. The initial conditions, boundary conditions and the source terms

follow from the exact solution. We use the well-know Taylor-Hood element (P2-P1) for the fluid equation and the piecewise quadratic polynomials (P2) for the porous equation. To see the effect on the results by change of time steps, we fix the diameter $h = 100$ for space triangulation. We apply the DLN algorithm to this test problem for 40 time steps and introduce the timestep function similar to that in [6]:

$$k_n = \begin{cases} 0.1 & 0 \leq n \leq 10, \\ 0.1 + 0.05 \sin(10t_n) & n > 10. \end{cases} \quad (5.1)$$

The graph of the time step function (5.1) is given in Figure 5.1. Figure 5.2 shows the speed contours and

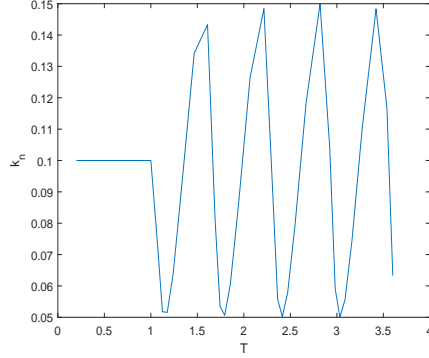


FIG. 5.1. Change of step size k_n .

velocity streamlines with parameter $\theta = 0.2, 0.5, 0.7$ respectively. From the graphs in Figure 5.2, we observe that good performance can be obtained for all three cases. Figure 5.3(a) and Figure 5.3(b) respectively show the comparison between the approximate solutions and the true solutions of the incompressible fluid velocity \mathbf{u}_f and porous media fluid hydraulic head ϕ with different θ . The variable timestepping DLN algorithm approximate exact solutions well, which confirms the stability of the DLN algorithm.

5.2. Test of constant Timestepping DLN algorithm. For constant timestep test, we refer to the numerical example in [30]. Let the computational domain Ω be composed of $\Omega_f = (0, 1) \times (1, 2)$ and $\Omega_p = (0, 1) \times (0, 1)$ with the interface $\Gamma = (0, 1) \times \{1\}$. We set the total time $T = 1$. The exact solution is:

$$\begin{aligned} \mathbf{u}_f &= \left((x^2(y-1)^2 + y) \cos(t), -\frac{2}{3}x(y-1)^3 \cos(t) + (2 - \pi \sin(\pi x)) \cos(t) \right), \\ p &= (2 - \pi \sin(\pi x)) \sin\left(\frac{1}{2}\pi y\right) \cos(t), \\ \phi &= (2 - \pi \sin(\pi x)) (1 - y - \cos(\pi y)) \cos(t). \end{aligned}$$

For this test, MINI (P1b-P1) space and piecewise linear polynomials (P1) space are used for the approximation of the incompressible fluid and the porous equation respectively. To confirm the consistency of the DLN algorithm, we set $h = \Delta t$ and calculate the errors and convergence rates for the functions \mathbf{u}_f , ϕ and p . The rate of convergence r is calculated by

$$r = \ln(e(\Delta t_1)/e(\Delta t_2))/\ln(\Delta t_1/\Delta t_2),$$

where $e(\Delta t)$ is the error computed by the DLN algorithm with time stepsize Δt .

Table 5.1, 5.2 and 5.3 show the fluid velocity \mathbf{u}_f , hydraulic head ϕ and pressure p errors of the DLN algorithm when $\theta = 0.2, 0.5, 0.7$. The results are almost the same for three different θ , but as θ increases, the errors of \mathbf{u}_f decrease slightly, while the errors of ϕ increase. Thus how to choose the best parameters leaves an open question. Moreover Table 5.4, Table 5.5 and Table 5.6 show the convergence rate of velocity \mathbf{u}_f , hydraulic head ϕ and pressure p with different θ and therefore verify the second-order convergence of the

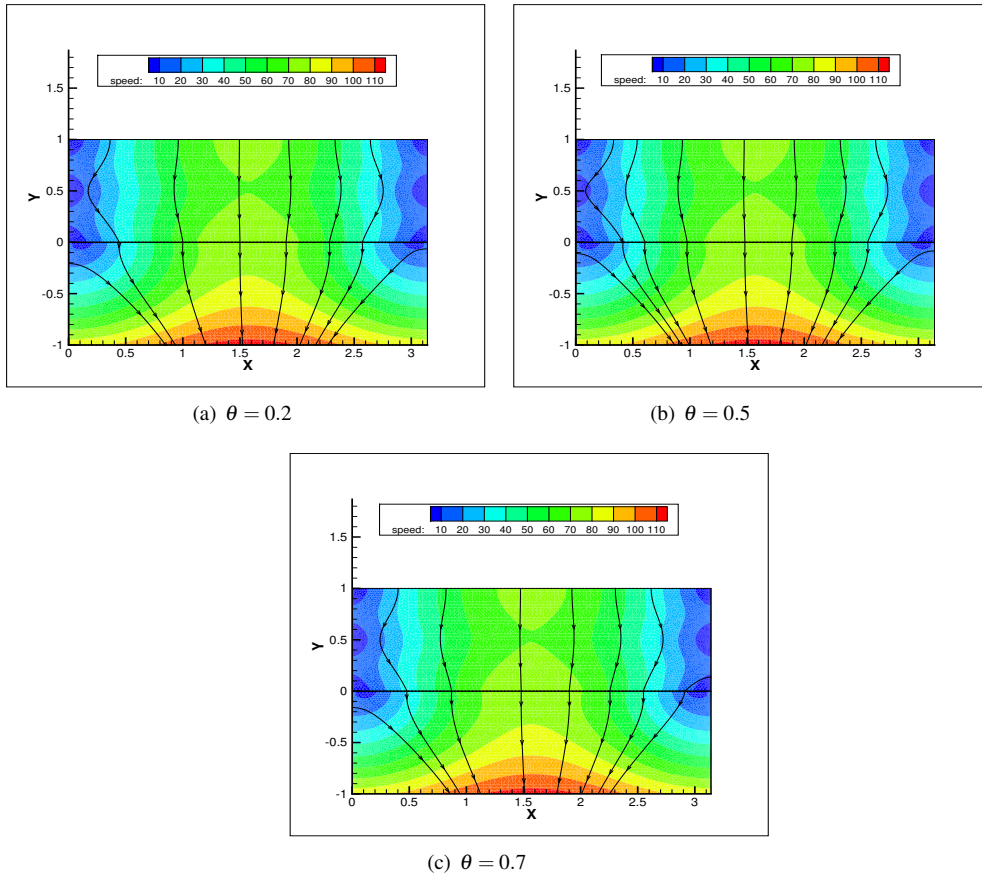


FIG. 5.2. The speed contours and velocity streamlines with $\theta = 0.2, 0.5, 0.7$.

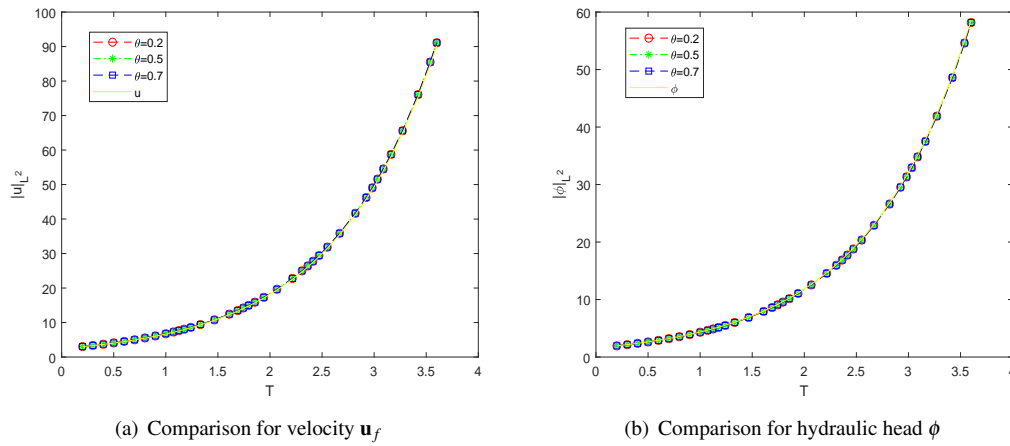


FIG. 5.3. Comparison between the approximate solutions and the exact solutions with different parameter θ .

DLN algorithm. Finally, Table 5.7 shows the corresponding errors obtained by the common BDF2 method. By comparison, we can see that the DLN algorithm obtains a better hydraulic head ϕ than BDF2 method.

$\Delta t = h$	$\ \mathbf{e}_{\mathbf{u}_f}\ _{2,0}$	$\ \mathbf{e}_{\mathbf{u}_f}\ _{2,1}$	$\ \mathbf{e}_\phi\ _{2,0}$	$\ \mathbf{e}_\phi\ _{2,1}$	$\ e_p\ _{2,0}$
1/10	0.0163655	0.599657	0.0143625	0.552125	0.175753
1/16	0.00657067	0.354318	0.00587243	0.359717	0.0785158
1/22	0.00353871	0.255182	0.00317754	0.268333	0.0490189
1/28	0.00218857	0.191492	0.00198363	0.2117	0.0306542
1/34	0.00150194	0.160602	0.00135819	0.177254	0.0213342

Table 5.1: The errors for DLN scheme with $\theta = 0.2$.

$\Delta t = h$	$\ \mathbf{e}_{\mathbf{u}_f}\ _{2,0}$	$\ \mathbf{e}_{\mathbf{u}_f}\ _{2,1}$	$\ \mathbf{e}_\phi\ _{2,0}$	$\ \mathbf{e}_\phi\ _{2,1}$	$\ e_p\ _{2,0}$
1/10	0.01615	0.506002	0.0146238	0.551755	0.138243
1/16	0.00652393	0.311263	0.00599802	0.359655	0.0637115
1/22	0.00351853	0.22917	0.00324735	0.268314	0.04083
1/28	0.00218086	0.176397	0.00202875	0.211693	0.0260884
1/34	0.00149633	0.148517	0.0013883	0.177249	0.0184629

Table 5.2: The errors for DLN scheme with $\theta = 0.5$.

$\Delta t = h$	$\ \mathbf{e}_{\mathbf{u}_f}\ _{2,0}$	$\ \mathbf{e}_{\mathbf{u}_f}\ _{2,1}$	$\ \mathbf{e}_\phi\ _{2,0}$	$\ \mathbf{e}_\phi\ _{2,1}$	$\ e_p\ _{2,0}$
1/10	0.0161161	0.488013	0.0150263	0.551591	0.128276
1/16	0.00652022	0.30443	0.00616699	0.359622	0.0604363
1/22	0.00351759	0.225303	0.00333733	0.268301	0.0393132
1/28	0.00218125	0.174198	0.00208573	0.211687	0.0252779
1/34	0.00149674	0.14679	0.00142616	0.177246	0.0179642

Table 5.3: The errors for DLN scheme with $\theta = 0.7$.

$\Delta t = h$	$r_{\mathbf{u}_f,0}$	$r_{\mathbf{u}_f,1}$	$r_{\phi,0}$	$r_{\phi,1}$	$r_{p,0}$
1/10	-	-	-	-	-
1/16	1.9416	1.11949	1.90286	0.911604	1.71441
1/22	1.94331	1.03066	1.92857	0.920353	1.47931
1/28	1.99249	1.19062	1.95378	0.982976	1.94657
1/34	1.93911	0.906045	1.9509	0.914669	1.86683

Table 5.4: The convergence order of errors for DLN scheme with $\theta = 0.2$.

$\Delta t = h$	$r_{\mathbf{u}_f,0}$	$r_{\mathbf{u}_f,1}$	$r_{\phi,0}$	$r_{\phi,1}$	$r_{p,0}$
1/10	-	-	-	-	-
1/16	1.92895	1.03382	1.8962	0.910541	1.64818
1/22	1.93885	0.961447	1.92678	0.920035	1.39722
1/28	1.98342	1.08527	1.95063	0.982834	1.85737
1/34	1.94019	0.886068	1.9538	0.914617	1.78066

Table 5.5: The convergence order of errors for DLN scheme with $\theta = 0.5$.

$\Delta t = h$	$r_{\mathbf{u}_f,0}$	$r_{\mathbf{u}_f,1}$	$r_{\phi,0}$	$r_{\phi,1}$	$r_{p,0}$
1/10	-	-	-	-	-
1/16	1.92532	1.00404	1.89485	0.910111	1.60126
1/22	1.93791	0.945172	1.92819	0.919886	1.35037
1/28	1.98157	1.06674	1.94911	0.982746	1.83126
1/34	1.93971	0.881715	1.95786	0.914595	1.75915

Table 5.6: The convergence order of errors for DLN scheme with $\theta = 0.7$.

$\Delta t = h$	$\ \mathbf{e}_{\mathbf{u}_f}\ _{2,0}$	$\ \mathbf{e}_{\mathbf{u}_f}\ _{2,1}$	$\ \mathbf{e}_{\phi}\ _{2,0}$	$\ \mathbf{e}_{\phi}\ _{2,1}$	$\ e_p\ _{2,0}$
1/10	0.0160291	0.450396	0.0165148	0.551278	0.116047
1/16	0.00650765	0.290462	0.00680715	0.359553	0.0561277
1/22	0.00351566	0.2176	0.0036845	0.268273	0.0373131
1/28	0.00218218	0.169732	0.00230674	0.211677	0.024088
1/34	0.00149872	0.143413	0.00157485	0.177236	0.0171673

Table 5.7: The errors for BDF2 scheme.

6. Conclusions. This report has shown that the DLN algorithm has advantages on variable timestepping analysis for the unsteady Stokes/Darcy model due to unconditional, long time G -stability and second order accuracy under variable time steps. Stability of the approximate solutions are obtained by G -stability of the DLN algorithm and second order accuracy of the numerical simulations are derived from combination of G -stability and consistency properties of the DLN algorithm. Therefore the variable time stepping algorithm would be popular if the complexity of the DLN algorithm is overcome. One efficient way would be implementation of the DLN algorithm through adding time filters on certain first order implicit method. Moreover, adaptivity process for the DLN algorithm would highly reduce the computation cost if reliable estimators of local truncation error can be obtained.

REFERENCES

- [1] Todd Arbogast and Mario San Martin Gomez, *A discretization and multigrid solver for a Darcy–Stokes system of three dimensional vuggy porous media*, Computational Geosciences **13** (2009), no. 3, 331–348.
- [2] Lori Badea, Marco Discacciati, and Alfio Quarteroni, *Numerical analysis of the Navier–Stokes/Darcy coupling*, Numerische Mathematik **115** (2010), no. 2, 195–227.
- [3] Yanzhao Cao, Max Gunzburger, Xiaoming He, and Xiaoming Wang, *Parallel, non-iterative, multi-physics domain decomposition methods for time-dependent Stokes–Darcy systems*, Mathematics of Computation **83** (2014), no. 288, 1617–1644.
- [4] A Çeşmelioglu and Béatrice Rivière, *Analysis of time-dependent Navier–Stokes flow coupled with Darcy flow*, Journal of Numerical Mathematics **16** (2008), no. 4, 249–280.
- [5] Ayçıl Çeşmelioglu and Béatrice Rivière, *Primal discontinuous Galerkin methods for time-dependent coupled surface and sub-surface flow*, Journal of Scientific Computing **40** (2009), no. 1-3, 115–140.
- [6] Robin Chen, William Layton, and Michael McLaughlin, *Analysis of variable-step/non-autonomous artificial compression methods*, Journal of Mathematical Fluid Mechanics **21** (2019).
- [7] Wenbin Chen, Max Gunzburger, Dong Sun, and Xiaoming Wang, *Efficient and long-time accurate second-order methods for the Stokes–Darcy system*, SIAM Journal on Numerical Analysis **51** (2013), no. 5, 2563–2584.
- [8] ———, *An efficient and long-time accurate third-order algorithm for the Stokes–Darcy system*, Numerische Mathematik **134** (2016), no. 4, 857–879.
- [9] G Dahlquist, *Positive functions and some applications to stability questions for numerical methods. recent advances in numerical analysis*, Proc. Symp., Madison/Wis, 1978.
- [10] Germud Dahlquist, *On the relation of G -stability to other stability concepts for linear multistep methods*, Tech. report, CM-P00069426, 1976.
- [11] Germund Dahlquist, *G -stability is equivalent to A -stability*, BIT Numerical Mathematics **18** (1978), no. 4, 384–401.
- [12] Germund G. Dahlquist, Werner Liniger, and Olavi Nevanlinna, *Stability of two-step methods for variable integration steps*, SIAM Journal on Numerical Analysis **20** (1983), no. 5, 1071–1085.
- [13] Marco Discacciati, Edie Miglio, and Alfio Quarteroni, *Mathematical and numerical models for coupling surface and groundwater flows*, Applied Numerical Mathematics **43** (2002), no. 1-2, 57–74.
- [14] VJ Ervin, EW Jenkins, and Shuyu Sun, *Coupled generalized nonlinear Stokes flow with flow through a porous medium*, SIAM Journal on Numerical Analysis **47** (2009), no. 2, 929–952.
- [15] Wenqiang Feng, Xiaoming He, Zhu Wang, and Xu Zhang, *Non-iterative domain decomposition methods for a non-stationary*

- Stokes–Darcy model with Beavers–Joseph interface condition*, Applied Mathematics and Computation **219** (2012), no. 2, 453–463.
- [16] Vivette Girault and Béatrice Rivière, *DG approximation of coupled Navier–Stokes and Darcy equations by Beaver–Joseph–Saffman interface condition*, SIAM Journal on Numerical Analysis **47** (2009), no. 3, 2052–2089.
- [17] DU Guangzhi and ZUO Liyun, *Local and parallel finite element method for the mixed Navier–Stokes/Darcy model with Beavers–Joseph interface conditions*, Acta Mathematica Scientia **37** (2017), no. 5, 1331–1347.
- [18] Ahmet Baris Guzel and William J. Layton, *Time filters increase accuracy of the fully implicit method*, BIT Numerical Mathematics **58** (2018), 301–315.
- [19] E. Hairer, S.P. Nørsett, and G. Wanner, *Solving ordinary differential equations II: Stiff and differential-algebraic problems*, Solving Ordinary Differential Equations, Springer, 1993.
- [20] Xiaoming He, Jian Li, Yanping Lin, and Ju Ming, *A domain decomposition method for the steady-state Navier–Stokes–Darcy model with Beavers–Joseph interface condition*, SIAM Journal on Scientific Computing **37** (2015), no. 5, S264–S290.
- [21] Yanren Hou, *Optimal error estimates of a decoupled scheme based on two-grid finite element for mixed Stokes–Darcy model*, Applied Mathematics Letters **57** (2016), 90–96.
- [22] Yanren Hou and Yi Qin, *On the solution of coupled Stokes/Darcy model with Beavers–Joseph interface condition*, Computers & Mathematics with Applications **77** (2019), no. 1, 50–65.
- [23] Nan Jiang and Changxin Qiu, *An efficient ensemble algorithm for numerical approximation of stochastic Stokes–Darcy equations*, Computer Methods in Applied Mechanics and Engineering **343** (2019), 249–275.
- [24] Guido Kanschat and Béatrice Riviere, *A strongly conservative finite element method for the coupling of Stokes and Darcy flow*, Journal of Computational Physics **229** (2010), no. 17, 5933–5943.
- [25] William Layton and Michael McLaughlin, *Doubly-adaptive artificial compression methods for incompressible flow*, arXiv e-prints (2019), arXiv:1907.08235.
- [26] William Layton, Wenlong Pei, Yi Qin, and Catalin Trenchea, *Analysis of the variable step method of Dahlquist, Liniger and Nevanlinna for fluid flow*, arXiv e-prints (2020), arXiv:2001.08640.
- [27] William Layton and Catalin Trenchea, *Stability of two IMEX methods, CNLF and BDF2-AB2, for uncoupling systems of evolution equations*, Applied Numerical Mathematics **62** (2012), no. 2, 112–120.
- [28] William J Layton, Friedhelm Schieweck, and Ivan Yotov, *Coupling fluid flow with porous media flow*, SIAM Journal on Numerical Analysis **40** (2002), no. 6, 2195–2218.
- [29] Yi Li and Yanren Hou, *A second-order partitioned method with different subdomain time steps for the evolutionary Stokes–Darcy system*, Mathematical Methods in the Applied Sciences **41** (2018), no. 5, 2178–2208.
- [30] Mo Mu and Xiaohong Zhu, *Decoupled schemes for a non-stationary mixed Stokes–Darcy model*, Mathematics of Computation **79** (2010), no. 270, 707–731.
- [31] Yi Qin and Yanren Hou, *Optimal error estimates of a decoupled scheme based on two-grid finite element for mixed Navier–Stokes/Darcy model*, Acta Mathematica Scientia **38** (2018), no. 4, 1361–1369.
- [32] ———, *The time filter for the non-stationary coupled Stokes/Darcy model*, Applied Numerical Mathematics **146** (2019), 260–275.
- [33] Yi Qin, Yanren Hou, Pengzhan Huang, and Yongshuai Wang, *Numerical analysis of two grad–div stabilization methods for the time-dependent Stokes/Darcy model*, Computers & Mathematics with Applications **79** (2020), no. 3, 817–832.
- [34] Béatrice Rivière, *Analysis of a discontinuous finite element method for the coupled Stokes and Darcy problems*, Journal of Scientific Computing **22** (2005), no. 1-3, 479–500.
- [35] Li Shan and Haibiao Zheng, *Partitioned time stepping method for fully evolutionary Stokes–Darcy flow with Beavers–Joseph interface conditions*, SIAM Journal on Numerical Analysis **51** (2013), no. 2, 813–839.
- [36] Li Shan, Haibiao Zheng, and William J Layton, *A decoupling method with different subdomain time steps for the nonstationary Stokes–Darcy model*, Numerical Methods for Partial Differential Equations **29** (2013), no. 2, 549–583.
- [37] Liyun Zuo and Guangzhi Du, *A multi-grid technique for coupling fluid flow with porous media flow*, Computers & Mathematics with Applications **75** (2018), no. 11, 4012–4021.
- [38] ———, *A parallel two-grid linearized method for the coupled Navier–Stokes–Darcy problem*, Numerical Algorithms **77** (2018), no. 1, 151–165.
- [39] Liyun Zuo and Yanren Hou, *A decoupling two-grid algorithm for the mixed Stokes–Darcy model with the Beavers–Joseph interface condition*, Numerical Methods for Partial Differential Equations **30** (2014), no. 3, 1066–1082.
- [40] ———, *Numerical analysis for the mixed Navier–Stokes and Darcy problem with the Beavers–Joseph interface condition*, Numerical Methods for Partial Differential Equations **31** (2015), no. 4, 1009–1030.
- [41] ———, *A two-grid decoupling method for the mixed Stokes–Darcy model*, Journal of Computational and Applied Mathematics **275** (2015), 139–147.